PROBABILISTIC THERMO-CHEMICAL ANLAYSIS OF A PULTRUDED COMPOSITE ROD

Ismet Baran[1*], Cem C. Tutum[1], Jesper H. Hattel[1]

[1]*Technical University of Denmark, Mechanical Engineering Department, DK-2800, Kgs. Lyngby. Denmark*
*isbar@mek.dtu.dk

Keywords: Probabilistic design, Pultrusion process, Computational simulation, curing.

Abstract
In the present study the deterministic thermo-chemical pultrusion simulation of a composite rod taken from the literature [7] is used as a validation case. The predicted centerline temperature and cure degree profiles of the rod match well with those in the literature [7]. Following the validation case, the probabilistic design of the pultrusion process, which has not been considered until now, is performed. The effect of statistical variations in the material (i.e. fiber and resin) and resin kinetic properties, as well as process parameters such as pulling speed and inlet temperature on the product quality (degree of cure) are examined by means of Monte Carlo Simulation (MCS) with Latin Hypercube Sampling (LHS) technique. The variations in the activation energy as well as the density of the resin are found to have a strong influence on the centerline degree of cure at the exit whereas the other process parameters have smaller influences. Moreover, different MCS options are examined to investigate their effects on the accuracy of the random output parameter.

1 Introduction

The pultrusion process is one of the most effective manufacturing techniques for production of composite materials having constant cross-sectional area. It has been widely used for manufacturing highly strengthened and continuous composite structures, e.g. wind turbine blades, ballistic resistance panels, spars of ship hulls, thin wall panel joiners, door/window frames, driveshaft of vehicles, etc. A schematic representation of the process can be seen in Fig. 1. Virtual manufacturing, in essence applying numerical process simulation, is an important step towards designing enduring and better-functioning products in the pultrusion process as well as in other manufacturing processes.
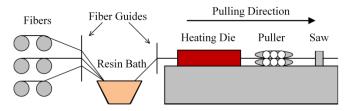

Figure 1. Schematic view of the pultrusion process. Fibers/mats and resin matrix are pulled together in the pultrusion direction by pullers through the heated die and then the cured composite is cut by a saw system.

There have been several numerical modeling studies specific to thermo-chemical simulation of the pultrusion process in the literature. Generally, the numerical techniques such as finite difference methods (FDM) and finite element methods (FEM) with control volume (CV) technique or nodal control volume (NCV) technique have been used for the simulation of the process [1-7]. However, these studies are limited by the deterministic prescription of the process and its material parameters. Probabilistic analyses of various engineering applications [8-12] have been investigated by using the probabilistic design system (PDS) toolbox of ANSYS.

This paper investigates the effects of uncertainties in the pultrusion process parameters (e.g. composite material properties, fiber volume ratio, pulling speed and pre-heating temperature) on the degree of cure at the die exit. The deterministic analysis is based on a thermo-chemical model of AS4/Epon 9420/9470/537 carbon-fiber/epoxy composite rod and it is performed for validation purpose by using both control volume based finite difference (CV/FD) method and the finite element with nodal control volume (FE/NCV) method. The temperature and the degree of cure profiles are in good agreement with experimental and simulation data taken from the literature [7]. For the probabilistic analysis, Monte Carlo simulations (MCS) with the Latin Hypercube Sampling (LHS) technique have been performed. For this purpose the PDS (Probabilistic Design System) Toolbox of ANSYS is utilized incorporating with a parametric deterministic model prepared with its own scripting language, APDL (ANSYS Parametric Design Language). This approach gives a better understanding of the effect of the variations inherently involved in the process and makes it easier or more practical to predict how large and sensitive the scatter of the output parameters (e.g. degree of cure) with respect to scatter in the input design parameters (i.e. randomly varying -probabilistic- input parameters with a given mean and standard deviation) are. In other words, this gives an evaluation of the robustness of the model.

2 Governing Equations

2.1 Energy Equation

The transient heat transfer equation in a cylindrical coordinate system for the composite rod can be written as

$$\rho Cp\left(\frac{\partial T}{\partial t}+u\frac{\partial T}{\partial z}\right)=k_z\frac{\partial^2 T}{\partial z^2}+\frac{k_r}{r}\frac{\partial}{\partial r}\left(r\frac{\partial T}{\partial r}\right)+(1-V_f)\rho_r Q \tag{1}$$

where T is the temperature, u is the pulling speed, t is the time, ρ is the density, Cp is the specific heat, k_z and k_r are the thermal conductivities in the axial direction (z) and in the radial direction (r) respectively. The internal heat generation [W/m^3] due to the exothermic reaction of the epoxy resin is expressed as $(1-V_f)\rho_r Q$ in Eq. 1 where V_f is the fiber volume ratio and Q is the specific heat generation rate [W/kg] due to the resin exothermic cure reaction. Lumped material properties are used and assumed to be constant. Similarly the steady state energy equation can be obtained by neglecting the time dependent term in Eq. 1, i.e. $\partial T/\partial t=0$.

2.2 Resin Kinetics

The curing of the thermosetting resin (here epoxy) is highly dependent on the exothermic chemical reaction inside the heating die. Generally the rate of resin reaction (R_r) which can also be expressed as the rate of the cure degree, is a function of temperature (T) and the degree of cure (α) itself. The degree of cure can be written as the ratio of the amount of heat generated ($H(t)$) during curing, to the total heat of reaction H_{tr}, i.e. $\alpha= H(t)/ H_{tr}$. R_r can be written as an Arrhenius type equation [3],

$$R_r(\alpha) = \frac{d\alpha}{dt} = \frac{1}{H_{tr}}\frac{dH(t)}{dt} = K_o \exp(-\frac{E}{RT})(1-\alpha)^n \qquad (2)$$

where K_o is the pre-exponential constant, E is the activation energy, R is the universal gas constant and n is the order of reaction (kinetic exponent). Ko, E, H_{tr} and n can be obtained by curve fitting procedure applied to the experimental data evaluated using a differential scanning calorimeter (DSC) [7]. As a result, Q (in Eq. 1) can be expressed as

$$Q = \frac{dH(t)}{dt} = H_{tr}R_r(\alpha) \qquad (3)$$

The rate of cure degree is derived from the chain rule and can be expressed as,

$$\frac{\partial \alpha}{\partial t} = R_r(\alpha) - u\frac{\partial \alpha}{\partial z} \qquad (4)$$

where it is the expression in Eq. 4 which is used as an output variable together with the temperature distribution in the numerical model.

3 Numerical Implementation
The deterministic thermo-chemical simulation of the pultrusion process is performed by using the CV/FD method (for the transient and the steady state solutions) [13] and the FE/NCV method (only for the steady state solution) separately in the validation case. However, the probabilistic analysis is carried out by using numerical model based on the FE/NCV technique. MATLAB [14] mathematical computing environment and ANSYS [15] are used for the implementation of the CV/FD and FE/NCV methods, respectively. In both methods, the internal heat generation together with the resin kinetics equation (Eq. 4) is coupled with the energy equation in an explicit manner in order to obtain a stable and fast numerical procedure since the internal heat generation is highly nonlinear (Eq. 1). The degree of cure is subsequently updated explicitly for each control volume using Eq. 4 in its discretized form.

The alternating direction implicit (ADI) method is implemented for the transient simulation of the pultrusion process performed by using the CV/FD method. Similarly the CV/FD steady state numerical scheme of the energy equation is obtained by discarding the time dependent terms used in the ADI scheme. In the CV/FD numerical schemes the total thermal resistances (K/W) being the sum of the single resistances coupled in series between the two adjacent control volumes are used [13]. The *upwind scheme* is used for the convective term ($u\partial T/\partial x$) in the energy equation and for the space discretization of the cure degree ($u\partial\alpha/\partial x$) in the resin kinetics equation in order to obtain a stable solution. The FE/NCV method, which is well documented in the lieature [2,3] is implemented for the steady state pultrusion simulation of the composite rod by using APDL. The degree of cure as well as the internal heat generation is updated explicitly at each node, as mentioned before, according to the obtained steady state nodal temperature data from ANSYS.

4 Validation Case: Deterministic Analysis
4.1 Problem Description
The deterministic thermo-chemical pultrusion simulation of a composite rod taken from the literature [7] is performed as a validation case. The temperature and the cure degree distributions are predicted with a given die wall temperature profile based on the experimental

work of Valliappan et al. [7]. The model geometry and the boundary conditions are shown in Fig. 2 (left). An axi-symmetrical model is used since the die wall temperature profile ($T_w(z)$) is assumed to be constant throughout the periphery of the rod. The graphite fiber reinforcement (Hercules AS4-12K) and epoxy resin (SHELL EPON9420/9470/537) system are used for the composite. The thermo-physical properties of the composite are given in Fig 2 (right). The resin kinetic parameters are [7]: H_{tr} = 323700 (J/kg), K_o = 191400 (1/s), E = 60500 (J/mol) and n = 1.69. The preheating temperature of the composite rod, i.e. T_{left}, is taken as the resin bath temperature ($\square$38 ^{o}C). The initial temperature is taken as 27 ^{o}C (ambient temperature) for the transient simulation. The initial cure degree of the composite is taken as 0 for both transient and steady state simulations. The convergence limits of the temperature and the degree of cure for both the transient and the steady state solutions are set to 0.001 ^{o}C and 0.0001, respectively.

Material	ρ (kg/m³)	Cp (J/kg K)	k_z (W/m K)	k_r (W/m K)
Epoxy Resin	1260	1255	0.2	0.2
Graphite	1790	712	66.0	11.6
Lumped (V_f = 62.2%)	1589.66	874.69	0.6628	0.6416

Figure 2. Schematic view of the pultrusion process of the composite rod and the corresponding boundary conditions (left). Material properties of the composite rod (right).

4.2 Results and Discussion

The transient and the steady state temperature and cure degree distributions are obtained for the deterministic model with a pulling speed of 30 cm/min (5 mm/s). The centerline temperature and cure degree profiles, which are predicted by using the CV/FD method and the FE/NCV method, are given in Fig. 3. It is seen that both the transient and the steady state results agree well with those in [7]. This shows that the utilized methods are stable and converged to a reliable solution. It is seen in Fig. 3 that after around 380 mm from the die inlet, the centerline temperature of the composite becomes higher than the die wall temperature due to the internal heat generation and the peak temperature of the composite is around 205 ^{o}C. The centerline exit cure degree is calculated as 0.844.
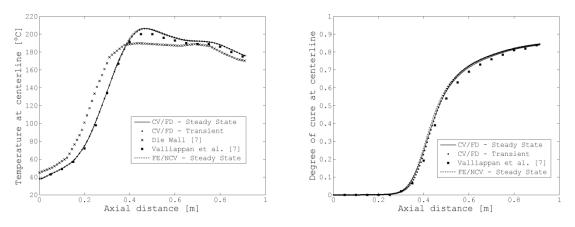

Figure 3. Predicted temperature (left) and cure degree profiles (right) at the centerline of the composite rod.

5 Probabilistic Analysis

5.1 Probabilistic Analysis Method

In the present work, the MCS technique is utilized since it is the most common and traditional technique for uncertainty or probabilistic analyses [15]. The LHS is selected for the sampling

method due to its superior sampling efficiency which means that it avoids overlapping samples (as could be the case in random sampling) that have been evaluated in the MCS loop and also forces the tails of a distribution to participate in the sampling process [9]. Assuming the deterministic model is correct; the MCS method converges to the true and correct probabilistic results with an increasing number of samples [8]. Besides, the MCS method does not use any assumptions or simplifications on the input/output parameters which makes it easy to use. The disadvantage of the MCS method is its computational cost.

5.2. Description of the Probabilistic Model
For the probabilistic analysis of the pultrusion process, the pulling speed, fiber volume ratio, inlet temperature, all the characteristic material properties and the resin kinetic parameters are considered as the random input parameters (RIPs). Table 1 summarizes the total of 14 RIPs and their distribution. Here, 'GAUSS' denotes the Gaussian (Normal) distribution with mean (μ) and standard deviation (σ) where the standard deviation (σ) is the multiplication of the mean (μ) and the coefficient of variation (COV), i.e. σ = μ×COV. In general, the statistical characteristics are obtained from the extensive data collection and data analysis. In the present study, the mean values of the RIPs are taken from the deterministic analysis and the standard deviations are estimated based on the engineering intuition. The first three RIPs (process parameters) are more controllable than the material properties, i.e. RIPs between 4-10th (Table 1), and hence the COVs of the first three RIPs are selected lower than the COVs of the RIPs between 4-10th. The last four RIPs are related with the resin kinetic parameters which are obtained from a curve fitting procedure of the DSC data where the deviation from the fitting may exist [16,17] (i.e 0.01 is used in this work). The centreline degree of cure at the exit (CDOCE) is taken as the random output response since it directly affects the expected mechanical properties of the product as well as the possibility of the defects.

Nr.	Property	Symbol	Unit	μ	COV	Distribution
1	Pulling speed	u	cm/min	30	0.02	GAUSS
2	Fiber volume ratio	V_f	-	0.622	0.02	GAUSS
3	Inlet temperature	T_{left}	K	311	0.02	GAUSS
4	Density of resin	ρ_r	kg/m^3	1260	0.05	GAUSS
5	Density of fiber	ρ_f	kg/m^3	1790	0.05	GAUSS
6	Specific heat of resin	Cp_r	J/kg K	1255	0.05	GAUSS
7	Specific heat of fiber	Cp_f	J/kg K	712	0.05	GAUSS
8	Thermal conductivity of resin	k_r	W/m K	0.2	0.05	GAUSS
9	Thermal conductivity of fiber in *r*-axis	$(k_r)_f$	W/m K	11.6	0.05	GAUSS
10	Thermal conductivity of fiber in *z*-axis	$(k_z)_f$	W/m K	66.0	0.05	GAUSS
11	Total heat of reaction	H_{tr}	J/kg	323700	0.01	GAUSS
12	Pre-exponential constant	K_0	1/s	191400	0.01	GAUSS
13	Activation energy	E	J/mol	60500	0.01	GAUSS
14	Order of reaction	n	-	1.69	0.01	GAUSS

Table 1. Statistical characteristics of the random input parameters (RIPs) for the pultrusion process.

Two different probabilistic case studies are performed:
  a) Case-1: The first 10 RIPs are used for the MCS analysis where 1000 simulations (samples) have been performed based on three different MCS options to investigate their effects on the accuracy of the output parameter:
    Case-1a: 1000 simulations are divided into 1 repetition (cycle) such that 1000 samples are selected all at once by using the LHS technique.
    Case-1b: 1000 simulations are divided into 10 repetitions (cycles) such that the 1000

simulations are done in 100 simulations with 10 repetitions. This adds more randomness to the LHS procedure.

Case-1c: 1000 simulations are divided into 1 repetition (cycle) with the autostop option in which the MCS is terminated before the total simulations are done if the convergence criteria are met. The convergence criteria are 0.001 for both the mean and the standard deviation of the random output parameter.

b) Case-2: All the RIPs in Table 2 (total of 14) are used for the MCS analysis where 1000 samples have been performed according to the results of Case-1 based on the best MCS option found so far.

5.3 Results and Discussion: Case-1

In order to get statistical significance, a total of 10 separate MCS runs, i.e. 10×1000 simulations, are performed for Case-1 (i.e. for each option: Case-1a, Case-1b and Case-1c). The 10000 runs require about 80 h using 2.3 GHz quad-core processor. Table 2 shows the mean values of the linear correlation coefficients between the RIPs and the corresponding output parameter (the CDOCE) for 10 runs. It is seen that the mean values of the correlation coefficients are very close to each other for the three options of Case-1 which shows that the MCS analysis converged for 1000 samples. However the standard deviations of the 10 runs for these three options differ and are given in Table 3. Case-1b has the lowest standard deviation values for the 6 RIPs out of 10 such as u, V_f, ρ_f, ρ_r, Cp_f and Cp_r. This shows that Case-1b is more accurate than Case-1a and Case-1c since the LHS procedure is more random in Case-1b. The mean of the first three rows in Table 2 (correlation coefficients) is given at the last row of Table 2. The same correlation coefficients are also given as a bar plot in Fig. 4 (right). As seen from this plot, ρ_r has the highest (and the only) positive correlation coefficient (0.587) and the rest has a lower negative correlation with the CDOCE. The corresponding sensitivities are given in the pie chart in Fig. 4 (right) based on the correlation coefficients. The percentage values indicate how sensitive the CDOCE is with respect to statistical variations in the RIPs. It is seen that the RIPs such as ρ_r, u and V_f cover 66% of the effect on the CDOCE and the rest portion is made up by the remaining RIPs (a total of 7).

	u	V_f	$(k_z)_f$	$(k_r)_f$	k_r	ρ_f	ρ_r	Cp_f	Cp_r	T_{left}
Case-1a	-0.470	-0.491	-0.018	-0.018	-0.283	-0.284	0.590	-0.102	-0.086	-0.013
Case-1b	-0.470	-0.502	-0.009	-0.020	-0.273	-0.295	0.594	-0.108	-0.080	0.002
Case-1c	-0.468	-0.496	-0.008	-0.011	-0.260	-0.307	0.578	-0.105	-0.087	-0.022
MEAN	-0.470	-0.496	-0.012	-0.016	-0.272	-0.296	0.587	-0.105	-0.085	-0.011

Table 2. The mean values of the correlation coefficients between the RIPs and the random output parameter (centerline degree of cure at the exit (CDOCE)) for 10 runs based on each MCS options (Case-1a, Case1b and Case-1c) of Case-1.

	u	V_f	$(k_z)_f$	$(k_r)_f$	k_r	ρ_f	ρ_r	Cp_f	Cp_r	T_{left}
Case-1a	-4.31	-4.46	-151.81	-234.90	-11.93	-10.34	3.30	-28.24	-39.25	-118.55
Case-1b	-3.17	-1.49	-301.09	-214.99	-11.74	-3.48	1.83	-25.45	-31.83	1525.34
Case-1c	-6.28	-4.01	-479.34	-206.85	-9.18	-6.79	3.19	-37.10	-51.67	-264.34

Table 3. The standard deviations of the correlation coefficients between the RIPs and the random output parameter (centerline degree of cure at the exit (CDOCE)) for 10 runs based on each MCS options of Case-1. The standard deviation values are given in percentage (%) of the mean values.

The cumulative distribution function (CDF) [15, 18] of the CDOCE is shown in Fig. 4 (left) for 10 runs of each MCS option of Case-1. It is seen that the CDFs for all runs (3×10) are close to each other. The sampling range of the CDOCE is between around 0.823 and 0.869

(i.e. 0.844 in average with 0.7% standard deviation). The value of the CDF at each point indicates the probability of the CDOCE laying under the point. For instance, the probability of having the CDOCE less than 0.835 is around 5% and the probability of the CDOCE greater than 0.852 is around 10% (100-90=10%).
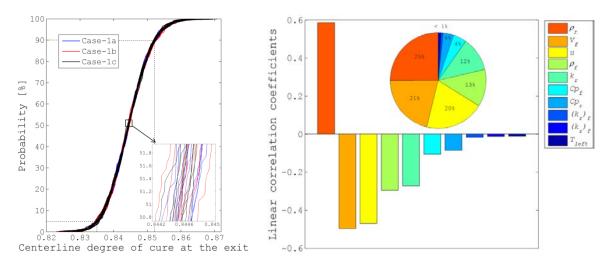

Figure 4. The CDFs of each option in Case-1 for 10 runs (left). The linear correlation coefficients (mean values of the three options in Case-1 for 10 runs) between the RIPs and the CDOCE in bar plot and corresponding sensitivities in pie chart (right).

5.4 Results and Discussion: Case-2

In Case-2, the MCS analysis is performed for 1000 samples based on the MCS option determined from Case-1b resulting in more accurate statistical results. The CDF is shown in Fig. 5 (left). The sampling range of the CDOCE is approximately between 0.725 and 0.915, which is wider than the range found in Case-1. The mean and the standard deviation of the CDOCE are calculated as 0.843 and 3.3%. The correlation coefficients between the RIPs (total of 14) and the CDOCE are given as a bar plot in Fig. 5 (right). It is seen that the *E* (activation energy) has the highest correlation coefficient (negative) and the magnitude is close to 1 (0.964) which indicates that the *E* is strongly correlated (i.e. inversely proportional) with the CDOCE. The corresponding sensitivities are given in a pie chart in Fig. 5 (right). The parameter *E* covers 57% of all the sensitivity distribution and the rest is sorted in a similar manner as in Case-1 (excluding resin kinetic parameters, i.e. n, K_0 and H_{tr}).
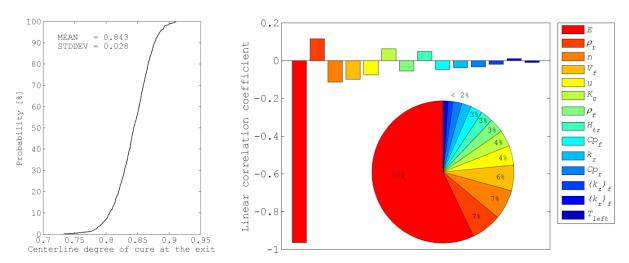

Figure 5. The CDF for Case-2 (left). The linear correlation coefficients between the RIPs and the CDOCE in bar plot and corresponding sensitivities in pie chart (right).

6 Conclusion

In the present work a deterministic thermo-chemical simulation for the pultrusion of a composite rod was developed and found to agree well with a validation case from the literature [7]. Two different probabilistic case studies were investigated by the application of the MCS technique with the LHS sampling in ANSYS PDS. In Case-1 the effects of the MCS options in ANSYS were investigated and it was found that the most accurate statistical results were obtained by dividing the total number of simulations (samples) into repetitions, i.e. total of 1000 simulations were done in 100 simulations with 10 repetitions within the LHS procedure. In Case-1 the variation in the density of the resin was found to have the most significant influence (positive correlation) on the CDOCE out of 10 RIPs. In Case-2, 14 RIPs were considered and it was found out that the variation in the activation energy of the resin has a very strong correlation (negative) with the CDOCE whereas the remaining RIPs have small influences on the CDOCE. So, it is very important that the resin system is characterized well regarding these two parameters.

References

[1] Joshi S.C., Chen X. Time-variant simulation of multi-material thermal pultrusion. *Appl Compos Mater*. **18**. pp. 283-296 (2010).

[2] Joshi S.C, Lam Y.C. Integrated approach for modelling cure and crystallization kinetics of different polymers in 3D pultrusion simulation. *J Mater Process Tech*. **174**. pp. 178-182 (2006).

[3] Liu X.L., Crouch I.G., Lam Y.C. Simulation of heat transfer and cure in pultrusion with a general-purpose finite element package. *Compos Sci Technol*. **60**. pp. 857-864 (2000).

[4] Liang G., Garg A., Chandrashekhara K. Cure characterization of pultruded soy-based composites. *J Reinf Plast Comp*. **24(14)**. pp. 1509-1520 (2005).

[5] Liu X.L. Numerical modeling on pultrusion of composite I beam. *Compos Part A-Appl S*. **32**. pp. 663-681 (2001).

[6] Roux J.A., Vaughan J.G., Shanku R., Arafat E.S., Bruce J.L., Johnson V.R. Comparison of measurements and modeling for pultrusion of a fiberglass/epoxy I-beam. *J Reinf Plast Comp*. **17**. pp. 1557-1578 (1998).

[7] Valliappan M., Roux J.A., Vaughan J.G., Arafat E.S. Die and post-die temperature and cure in graphite-epoxy composites. *Compos Part B-Eng*. **27**. pp. 1-9 (1996).

[8] Reh S., Beley J.D., Mukherjee S., Khor E.H. Probabilistic finite element analysis using ANSYS. *Struct Saf*. **28**. pp. 17-43 (2006).

[9] Cai B., Liu Y., Liu Z., Tian X., Ji R., Zhang Y. Probabilistic analysis of composite pressure vessel for subsea blowout preventers. *Eng Fail Anal*. **19**. pp. 97-108 (2012).

[10] Nakamura T., Fujii K. Probabilistic transient thermal analysis of an atmospheric reentry vehicle structure. *Aerosp Sci Technol*. **10**. pp. 346-354 (2006).

[11] Zhang Y., Qi Z., Lang X., Zhao M. Reliability Analysis of the Diamond Saw Blades Based on ANSYS. *Applied Mechanics and Materials*. **130-134**. pp. 887-890 (2012).

[12] Liu P.F., Zheng J.Y. Strength reliability analysis of aluminium-carbon fiber/epoxy composite laminates. *J Loss Prevent Proc*. **23**. pp. 421-427 (2010).

[13] Hattel J.H. Fundamentals of numerical modelling of casting processes. Polyteknisk Forlag. 1st Edition (2005).

[14] MATLAB (7.12.0.635) Reference Guide. The Mathworks Inc. (2011).

[15] User's manual of ANSYS 13.0, ANSYS Inc. (2010).

[16] He Y. DSC and DEA studies of underfill curing kinetics. *Thermochim Acta*. **367-368**. pp. 101-106 (2001).

[17] Wang J., Fang X., Wu M., He X., Liu W., Shen X. Synthesis, curing kinetics and thermal properties of bisphenol-AP-based benzoxazine. *Eur Polym J*. **47**. pp. 2158-2168 (2011).

[18] Kececioglu D. Reliability engineering handbook. vol. 2. (Upper Sadle River 07458. NJ): Prentice-Hall (1991).